Surface Chemistry

International Edition: DOI: 10.1002/anie.201802040
German Edition: DOI: 10.1002/ange.201802040

Higher Acenes by On-Surface Dehydrogenation: From Heptacene to Undecacene

Rafal Zuzak[+], Ruth Dorel[+], Marek Kolmer, Marek Szymonski, Szymon Godlewski, and Antonio M. Echavarren**

Abstract: *A unified approach to the synthesis of the series of higher acenes up to previously unreported undecacene has been developed through the on-surface dehydrogenation of partially saturated precursors. These molecules could be converted into the parent acenes by both atomic manipulation with the tip of a scanning tunneling and atomic force microscope (STM/AFM) as well as by on-surface annealing. The structure of the generated acenes has been visualized by high-resolution non-contact AFM imaging and the evolution of the transport gap with the increase of the number of fused benzene rings has been determined on the basis of scanning tunneling spectroscopy (STS) measurements.*

Acenes are a family of polycyclic aromatic hydrocarbons (PAHs) constituted by fused benzene rings disposed in a straight linear arrangement. They have captivated scientists for years on account of their unique properties,[1] which make them attractive for use in molecular electronics.[2] Furthermore, acenes can be also regarded as the narrowest graphene nanoribbons with zigzag edges, and therefore have potential applications in spintronics[3] and plasmonics.[4] The properties of acenes strongly depend on their size, thus expecting for the largest members of the series higher charge carrier mobilities, lower reorganization energies, and smaller HOMO–LUMO (highest occupied molecular orbital—lowest unoccupied molecular orbital) gaps.[2c,5] Nonetheless, the reactivity and therefore the instability of acenes also increases as the number of fused rings grows, which can be easily understood invoking the Clar's aromatic sextet rule.[6] On the other hand, theoretical calculations predict that the contribution of the open-shell singlet state to the electronic ground-state configuration shall rapidly grow for acenes containing more than 10 annulated rings,[7] yielding interesting magnetic and electronic properties and therefore making their synthesis and characterization quite appealing.

A common strategy to circumvent the intrinsic instability of higher acenes is the use of substituents directly attached to the aromatic core,[8] which has allowed the preparation of several stabilized derivatives of higher acenes up to nonacene.[9] In contrast, the synthesis and study of the non-functionalized hydrocarbons have constituted an enormous challenge until recently.[10] The photodecarbonylation of stable α-(diketo)precursors in solid matrices of noble gases allowed the generation of higher acenes up to nonacene.[11] Furthermore, both hexacene[12] and heptacene[13] could also be isolated in bulk by thermolysis of the corresponding carbonyl-bridged adduct and dimers, respectively.

The surface-assisted synthesis performed in ultra-high vacuum (UHV) conditions constitutes a powerful complementary tool to solution chemistry, thus enabling the preparation and stabilization of intrinsically unstable compounds. This approach pioneered in 2000 by Hla and co-workers[14] proved to be successful in the atomically precise generation of a range of covalent molecular architectures,[15] and more recently in the synthesis of new elusive compounds.[16] Furthermore, the development of new scanning tunneling and atomic force microscopy (STM/AFM) methods has not only allowed for detailed mapping of the molecules electronic structure,[17] but more importantly made the detailed structural imaging feasible providing an unprecedented resolution and precision.[18] The approach based on UHV deposition of stable derivatives on a crystalline substrate and subsequent transformation into target molecules has been successfully applied for synthesis of some members of the acene series. A pioneer example was described in 2013 for the synthesis of pentacene from tetrathienoanthracene on a Ni(111) surface.[19] In 2017 both heptacene[20] and heptacene organometallic complexes[21] were generated from α-diketone precursors on Ag(111) and Au(111), respectively. Furthermore, epoxyacenes have been used over the last two years to generate tetracene on Cu(111),[22] and hexacene[23] and decacene[24] on Au(111).

Hydroacenes—partially saturated acenes—were already described as "hydrogen-protected acenes" more than one

[*] R. Zuzak,[+] Dr. M. Kolmer, Prof. M. Szymonski, Dr. S. Godlewski
Centre for Nanometer-Scale Science and Advanced Materials
NANOSAM, Faculty of Physics, Astronomy
and Applied Computer Science
Jagiellonian University, Łojasiewicza 11, 30-348 Kraków (Poland)
E-mail: szymon.godlewski@uj.edu.pl
Dr. R. Dorel,[+] Prof. A. M. Echavarren
Institute of Chemical Research of Catalonia (ICIQ)
Barcelona Institute of Science and Technology
Av. Països Catalans 16, 43007 Tarragona (Spain)
E-mail: aechavarren@iciq.es
Prof. A. M. Echavarren
Departament de Química Orgànica i Analítica
Universitat Rovira i Virgil
C/Marcel·lí Domingo s/n, 43007 Tarragona (Spain)
[+] These authors contributed equally to this work.
Supporting information and the ORCID identification number(s) for the author(s) of this article can be found under: https://doi.org/10.1002/anie.201802040.

decade ago.[25] However, their use as direct precursors of the conjugated systems has been typically circumscribed to the preparation of acenes with up to five linearly fused benzene rings. We recently developed a general method for the synthesis of hydroacenes based on the gold(I)-catalyzed cyclization of aryl-tethered 1,7-enynes,[26] and successfully used tetrahydrononacene, one of the resulting partially saturated molecules, as a stable precursor for the synthesis and study of the properties of nonacene on a Au(111) surface.[27] On the basis of these results, we anticipated the development of a unified approach for the preparation and study of higher acenes on metallic surfaces, which could be extended for the synthesis of yet unknown even higher acenes. Herein we report the on-surface synthesis of the complete series from heptacene (**2**) up to previously unknown undecacene (**6**) through the dehydrogenation of the corresponding tetrahydroacene precursors **1** (Scheme 1). In order to confirm

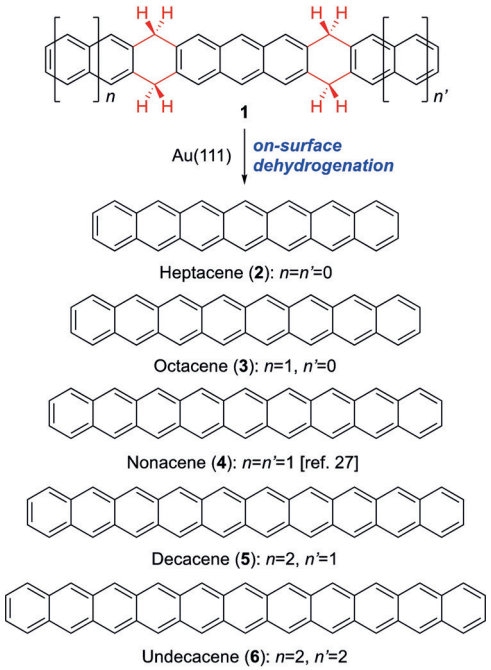

Scheme 1. Unified approach to higher acenes by on-surface dehydrogenation of hydroacenes.

the generation of intrinsically unstable higher acenes, high resolution nc-AFM imaging with a CO functionalized tip was applied,[18a] which provided doubtless structural and chemical identification of the synthesized compounds. The generation of the acene series was complemented by scanning tunneling spectroscopy (STS) measurements, which revealed the resonances associated with HOMO and LUMO orbitals and therefore allowed us to quantify the transport electronic gap evolution upon extension of the molecule board for acenes physisorbed on Au(111).

The synthesis of the tetrahydroacene precursors **1** was based on the double gold(I)-catalyzed cyclization of dienynes **8**,[26] which were assembled through the double Sonogashira cross-coupling between 1,4-diiodobenzene and terminal alkynes **7** (Scheme 2).[28] The double cyclization of **8** may

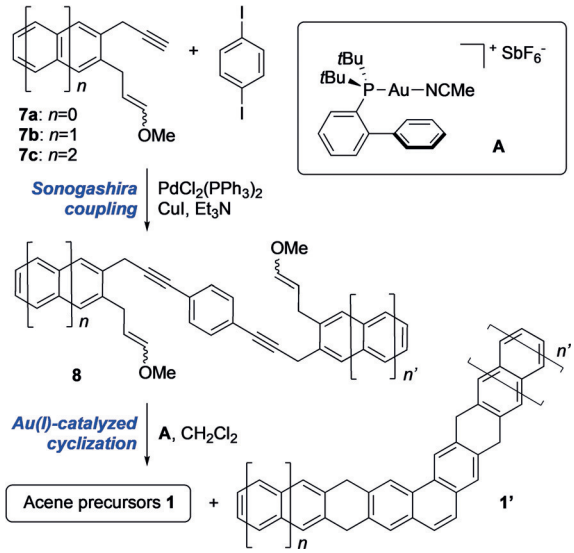

Scheme 2. Synthesis of tetrahydroacenes **1**.

give rise to the desired acene precursors **1** and their kinked isomers **1′** depending on the regioselectivity of the second cyclization. In the case of the cyclization of **8a** ($n=n'=0$), **8b** ($n=1$, $n'=0$), and **8c** ($n=n'=1$), the linear cyclization products **1a–c**—precursors of hepta- (**2**), octa- (**3**), and nonacene (**4**), respectively—can be easily separated from **1a–c′** due to their differences in solubility. In contrast, tetrahydrodecacene (**1d**) and tetrahydroundecacene (**1e**) exhibit a solubility comparable to their kinked counterparts **1d′** and **1e′** in a range of organic solvents, and consequently could not be isolated as single isomers. Therefore, mixtures of **1d**/**1d′** and **1e**/**1e′** were used in this study for the on-surface synthesis of the corresponding acenes.[28]

With the tetrahydroacenes **1a**,**b** and **1d**,**e** in hand, we next turned our attention to their application as precursors of the acene series by on-surface dehydrogenation following a procedure related to the one we previously developed for the preparation of nonacene from **1c**.[27] In general, parent acenes could be generated either thermally by annealing of the sample to 520 K for 10 minutes or by the application of the microscope tip.[28] The latter process could be performed locally with the tip apex located over the non-aromatic ring bearing two methylene groups. Increasing the applied bias voltage results in a dehydrogenation process accompanied with the aromatization and planarization of the molecular fragment subjected to manipulation. The threshold voltage for the dehydrogenation depends on the actual structure of the molecule.[27] However, we found that raising the bias voltage to 2.5 V was sufficient to carry out the dehydrogenation of all the investigated hydroacene compounds **1**. Furthermore, the tip-induced dehydrogenation process could also be achieved in a slightly different manner with the tip scanning across the surface at elevated bias voltage, which was found to be a competitive alternative to the thermal treatment and gave rise to the dehydrogenation of the majority of the physisorbed molecules. Nonetheless, the results herein presented mainly focus on the thermal treatment protocol due to its high efficiency in the simultaneous

dehydrogenation of an array of precursors. The tip-induced approach was also tested to confirm its applicability and is demonstrated for the synthesis of undecacene.[28]

Figure 1 illustrates the on-surface generation of higher acenes. Submonolayer coverage of **1a**, **1b** and **1d/1d′** was sublimed onto the Au(111) surface. Figure 1a shows the typical STM overview with mostly intact tetrahydroacene species, which are recognized in empty state images by their characteristic appearance with two pronounced lobes associated with the presence of four methylene groups per molecule. These lobes are also recognizable in the STM image profiles shown in Figure 1c. The precursors are preferentially located in the corners of the surface herringbone reconstruction similarly to the previously reported pentacene[29] and nonacene[27] molecules. With the increase of coverage, the molecules tend to follow the reconstruction pattern settling themselves mostly in-between the brighter appearing rows of the surface reconstruction. In STM images precursors **1a**, **1b** and **1d** could be easily discerned. Whereas intrinsically in all cases the separation of the two non-aromatic rings is identical and equals three benzene units located in-between, compound **1a** appears as the shortest with symmetrically located two bright lobes (Figure 1a, violet rectangle). In contrast, precursor **1b** appears slightly longer due to the extension of one terminus from a single benzene ring to the naphthalene moiety (Figure 1a, green rectangle). This is also evidenced by the elbow present in the left-hand side of the green cross section presented in Figure 1c. Compound **1d** is found as the longest precursor with clearly visible extended aromatic fragments observed at both termini of the molecule in the topographic image (Figure 1a, blue rectangle). This could also be noted in the blue cross section in Figure 1c. Apart from acene precursors **1a**,**b**,**d**, kinked species that we assign to **1d′** could also be visualized. A small amount of partially or completely dehydrogenated species (dihydroacenes and acenes, respectively) could also be found at this stage, as exemplified by the molecules in the white and red contours in Figure 1a. After annealing compounds **1** were converted into acenes as documented in the STM image shown in Figure 1b, which indicates the disappearance of the bright lobes attributed to the methylene moieties as previously observed for nonacene.[27] Vanishing of lobes could also be noted in the purple, grey and yellow profiles visualized in Figure 1c. Moreover, the behavior of the molecules during STM imaging differs between saturated precursors and parent acenes. Whereas some precursors **1** tend to relocate over the surface as indicated by white arrows in Figure 1a, a fraction of acenes could be characterized by a frustrated movement indicated by yellow arrows in Figure 1b and recorded as a noisy appearance of the termini, in agreement with the situation previously reported for nonacene molecules.[27] At first glance one can note by comparing Figure 1a and 1b that all molecules shown in Figure 1b have been converted into the corresponding conjugated acenes upon annealing, thus indicating that the dehydrogenation process is highly efficient, leading practically to almost 100% conversion rate.

Since simple STM imaging was not sufficient to discern the details of the atomic structure of adsorbates, we applied high resolution nc-AFM measurements with the probe tip

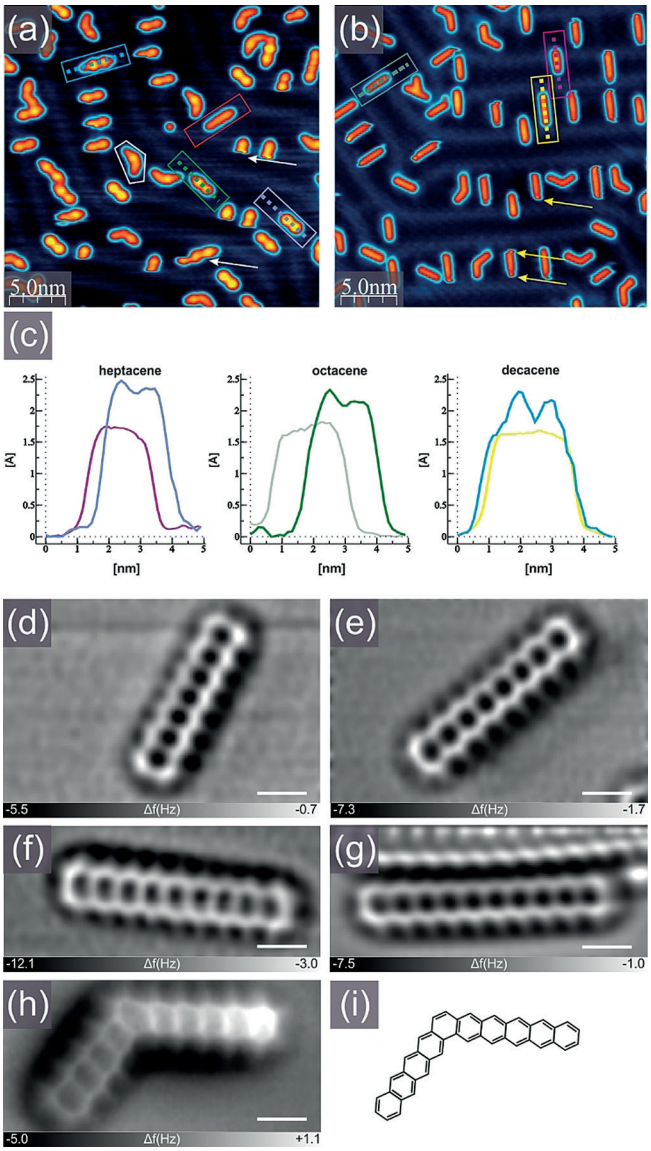

Figure 1. On-surface generation of higher acenes. a,b) Empty state STM images of the Au(111) surface partially covered with a) hydrogen-protected acene precursors **1a**, **1b**, and **1d**, and kinked isomer **1d′**, and b) heptacene (**2**), octacene (**3**), decacene (**5**) and kinked decacene isomer (**5′**). Precursor molecules are easily discernible by the presence of two pronounced lobes corresponding to two non-aromatic rings each containing two methylene groups, exemplary precursors are marked by rectangles: **1a**—violet, **1b**—green, **1d**—blue. Parent acenes in (b) are indicated by rectangles: **2**—purple, **3**—gray, **5**—yellow. Dashed lines in (a) and (b) indicate directions of profile lines shown in (c). After deposition a small fraction of molecules could be found already partially (white contour) or very rarely completely dehydrogenated (red rectangle). White and yellow arrows in (a) and (b) indicate the typical displacement of precursors and frustrated motion of acenes during STM imaging, respectively. Tunneling current 30 pA, bias voltage +2.0 V. c) Profile lines along precursor molecules and parent acenes showing a difference in their STM appearance and evidencing the presence of two pronounced lobes in the topographies of the precursors. d–h) Laplace filtered constant height, frequency shift nc-AFM images of **2** (d), **3** (e), **4** (f),[27] **5** (g), and **5′** (h) generated by annealing, scale bar: 5 Å. i) Structural scheme of **5′**.

functionalized with a CO molecule in order to doubtlessly prove formation of the series of parent acenes (Figure 1 d–g). Hence, submolecularly resolved nc-AFM images provided the ultimate insight into the chemical structure of the generated molecules. Detailed inspection of constant height frequency shift images indicates the presence of linearly fused benzene rings with single hydrogen termination of carbon atoms located in the elbows of the zig-zag edges, thus confirming formation of unsubstituted acenes. Additionally, we demonstrate that the bent species could be ascribed to the presence of kinked decacene isomer (**5′**) with discernible pentacene and tetracene moieties annulated at the angle of 120° by the central benzene ring (Figure 1 h–i).

The nc-AFM images plainly unveil the planarity of the entire acene series, which strongly supports relatively weak van der Waals-type interactions with the substrate without covalent linkage. This finding is further supported by the high mobility of the molecules on the surface, which allows for efficient planar displacement even at moderate bias voltages and low tunneling currents.[28] This behavior observed on Au(111) is in contrast to the recently reported increased interaction of the central part of heptacene molecules with the Ag(111) surface, which results in a distortion from the planar configuration.[20] The lack of covalent bonding with the Au(111) surface makes perspectives for spatial electronic mapping of nearly undistorted molecular orbitals,[27] but it also makes detailed imaging more challenging due to frequent unintentional tip-induced displacements of the molecules. We found that the immobilization of decacene molecules was particularly difficult to achieve, which may arise from their increased length compared to smaller homologs hindering from location between the elevated surface reconstruction rows. The above-mentioned location in-between the surface pattern has been observed preferentially for shorter acenes. Therefore, the high resolution nc-AFM image of a decacene molecule was recorded when the organic compound was immobilized in the vicinity of the surface step, as evidenced in the upper part of Figure 1 g.

After the successful preparation of the above-described acene series, we next embarked on the synthesis of previously unexplored undecacene, which constitutes the longest acene described to date, starting from a mixture of **1e**/**1e′**. The situation occurred to be remarkably different compared to the previously conducted experiments for shorter acenes. We immediately noted the presence of a considerable amount of kinked tetrahydroundecacene isomers **1e′** along with a significantly lower amount of linear **1e** molecules. In addition, smaller fragments were also located preferentially in the surface reconstruction pattern elbows, known for being more reactive. We attribute the presence of the latter compounds to the deposition of the fragmented undecacene precursors **1e**,[28] which is reasonable if we take into account the decrease in stability as the number of annulated rings increases.[30] Similarly, the decreased ratio of linear precursors to kinked ones could be rationalized considering the higher stability of the latter. Figure 2 a illustrates the Au(111) sample after deposition of **1e** and **1e′** species. In order to generate undecacene molecules we applied both approaches, on-surface annealing and tip-induced molecule manipulation.[28]

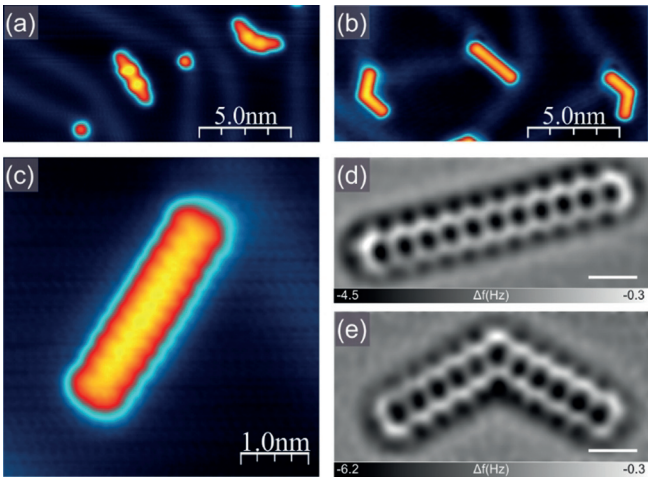

Figure 2. On-surface generation of undecacene (**6**). Empty state STM images of the Au(111) surface a) with the mixture of undecacene precursors **1e** and **1e′** and b) subsequently thermally generated parent **6** and kinked undecacene isomer **6′**. Tunneling current: a,b) 30 pA, c) 150 pA, bias voltage +2.0 V. c) High-resolution filled state STM image of **6** with eleven lobes visible along the molecule, tunneling current 30 pA, bias voltage −1.0 V. d–e) Present Laplace filtered constant height, frequency shift nc-AFM images of **6** (d) and **6′** (e); scale bar: 5 Å.

Figure 2 b shows the sample after annealing at 520 K for 10 minutes with clear disappearance of the previously observed pronounced lobes attributed to the methylene moieties of **1e** and **1e′**, thus indicating that the initial molecules have been dehydrogenated. The high-resolution STM image displayed in Figure 2 c indicates the presence of eleven lobes corresponding to the eleven linearly fused benzene rings of undecacene (**6**). In order to provide the ultimate confirmation of the generation of undecacene we performed high-resolution nc-AFM imaging (Figure 2 d). For the sake of completeness, the structure of the kinked undecacene isomer **6′** is shown in Figure 2 e.

The synthesis of the whole acene series provided a unique chance to analyze the dependence of the STS measured transport gap on the number of fused benzene rings. Figure 3 shows the results obtained in our study, including data previously reported for pentacene[29] and hexacene.[23] A simple and often used empirical equation links linearly the gap with the inverse number of fused benzene rings.[31] It shall be expected that for longer acenes the exponential decay of the gap with the number of annulated repeating units should better describe the trend and the saturation value.[32] However, in the analyzed range of only a few (5–10) fused benzene units, as indicated in Figure 3 a, both inverse proportionality (red line) and the exponential decay (blue line) could be well-fitted. In contrast, undecacene deviates toward larger gap values, which points towards the saturation of further band gap lowering for higher acenes. This trend is even better visualized in Figure 3 b, where the gap is drawn as a function of inversed number of annulated rings and clearly exhibits deviation from linearity for the longest acenes. These findings could be rationalized by the anticipated increased contribution of the open-shell configuration to the overall electronic configuration, which according to recent theoretical studies

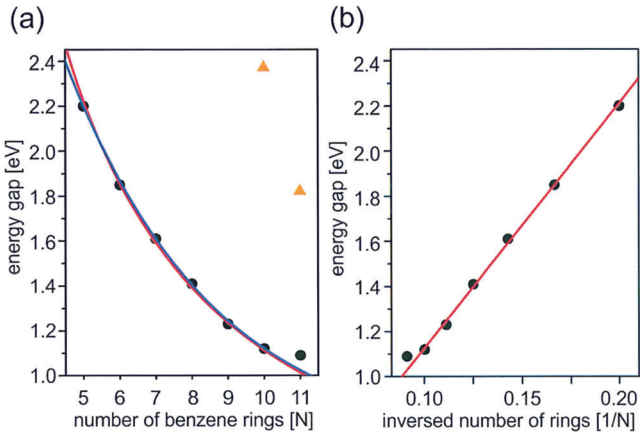

Figure 3. STS measured transport gap for long acenes on Au(111). a) Dependence of the gap on the number of fused benzene rings with the inverse proportionality fit (red curve) and exponential decay (blue curve) for pentacene–decacene data. Values recorded for kinked isomers are displayed by orange triangles.[28] b) Transport gap drawn as a function of the inversed number of rings with the linear fit for pentacene–decacene data. Gap values for pentacene[29] and hexacene[23] are taken from the literature.

are particularly important for acenes containing more than 10 rings.[7] The absolute gap values are affected by screening effects, which are known to induce renormalization.[33]

In summary, the complete series of higher acenes from heptacene up to previously unreported undecacene has been synthetized on a Au(111) surface through the dehydrogenation of tetrahydroacene precursors. The conjugated systems could be accessed both by surface annealing and tip-induced dehydrogenation. Unambiguous proof of their formation was obtained by high-resolution nc-AFM imaging. Furthermore, the evolution of the transport gap on the surface with the acene length was established on the basis of STS measurements. This work therefore showcases the versatility of hydroacenes as hydrogen-protected precursors of elusive higher acenes when combined with the on-surface synthesis toolbox, which gives future perspective for the study of even higher members of this intriguing family of PAHs.

Acknowledgements

This research was supported by the National Science Center, Poland (2017/26/E/ST3/00855), Agencia Estatal de Investigación (CTQ2016-75960-P MINECO/AEI/FEDER, UE, AEI-Severo Ochoa Excellence Accreditation 2014–2018, SEV-2013-0319), the European Research Council (advanced grant number 321066), the AGAUR (2017 SGR 1257), and CERCA Program/Generalitat de Catalunya. R.Z. acknowledges support received from the National Science Center, Poland (2017/24/T/ST5/00262).

Conflict of interest

The authors declare no conflict of interest.

Keywords: acenes · atomic force microscopy · dehydrogenation · surface chemistry · undecacene

How to cite: *Angew. Chem. Int. Ed.* **2018**, *57*, 10500–10505
Angew. Chem. **2018**, *130*, 10660–10665

[1] a) J. E. Anthony, *Angew. Chem. Int. Ed.* **2008**, *47*, 452–483; *Angew. Chem.* **2008**, *120*, 460–492; b) M. Watanabe, C.-Y. Chen, Y. J. Chang, T. J. Chow, *Acc. Chem. Res.* **2013**, *46*, 1606–1615.
[2] a) M. Bendikov, F. Wudl, D. F. Perepichka, *Chem. Rev.* **2004**, *104*, 4891–4946; b) J. E. Anthony, *Chem. Rev.* **2006**, *106*, 5028–5048; c) C. Wang, H. Dong, W. Hu, Y. Liu, D. Zhu, *Chem. Rev.* **2012**, *112*, 2208–2267; d) D. Xiang, X. Wang, C. Jia, T. Lee, X. Guo, *Chem. Rev.* **2016**, *116*, 4318–4440; e) Q. Ye, C. Chi, *Chem. Mater.* **2014**, *26*, 4046–4056.
[3] W. Han, R. K. Kawakami, M. Gmitra, J. Fabian, *Nat. Nanotechnol.* **2014**, *9*, 794–807.
[4] L. Bursi, A. Calzolari, S. Corni, E. Molinari, *ACS Photonics* **2014**, *1*, 1049–1058.
[5] a) K. N. Houk, P. S. Lee, M. Nendel, *J. Org. Chem.* **2001**, *66*, 5517–5521; b) Z. Sun, Q. Ye, C. Chi, J. Wu, *Chem. Soc. Rev.* **2012**, *41*, 7857–7889.
[6] E. Clar, *The Aromatic Sextet*, Wiley, London, **1972**.
[7] Y. Yang, E. R. Davidson, W. Yang, *Proc. Natl. Acad. Sci. USA* **2016**, *113*, E5098–E5107.
[8] a) K. J. Thorley, J. E. Anthony, *Isr. J. Chem.* **2014**, *54*, 642–649; b) C. Chi, X. Shi, *Chem. Rec.* **2016**, *16*, 1690–1700.
[9] a) S. S. Zade, M. Bendikov, *Angew. Chem. Int. Ed.* **2010**, *49*, 4012–4015; *Angew. Chem.* **2010**, *122*, 4104–4107; b) I. Kaur, M. Jazdzyk, N. N. Stein, P. Prusevich, G. P. Miller, *J. Am. Chem. Soc.* **2010**, *132*, 1261–1263; c) B. Purushothaman, M. Bruzek, S. R. Parkin, A.-F. Miller, J. E. Anthony, *Angew. Chem. Int. Ed.* **2011**, *50*, 7013–7017; *Angew. Chem.* **2011**, *123*, 7151–7155.
[10] a) H. F. Bettinger, C. Tönshoff, *Chem. Rec.* **2015**, *15*, 364–369; b) R. Dorel, A. M. Echavarren, *Eur. J. Org. Chem.* **2017**, 14–24.
[11] a) R. Mondal, R. M. Adhikari, B. K. Shah, D. C. Neckers, *Org. Lett.* **2007**, *9*, 2505–2508; b) R. Mondal, B. K. Shah, D. C. Neckers, *J. Am. Chem. Soc.* **2006**, *128*, 9612–9613; c) C. Tönshoff, H. F. Bettinger, *Angew. Chem. Int. Ed.* **2010**, *49*, 4125–4128; *Angew. Chem.* **2010**, *122*, 4219–4222.
[12] M. Watanabe, Y. J. Chang, S.-W. Liu, T.-H. Chao, K. Goto, M. M. Islam, C.-H. Yuan, Y.-T. Tao, T. Shinmyozu, T. J. Chow, *Nat. Chem.* **2012**, *4*, 574–578.
[13] R. Einholz, T. Fang, R. Berger, P. Grüninger, A. Früh, T. Chassé, R. F. Fink, H. F. Bettinger, *J. Am. Chem. Soc.* **2017**, *139*, 4435–4442.
[14] S.-W. Hla, L. Bartels, G. Meyer, K.-H. Rieder, *Phys. Rev. Lett.* **2000**, *85*, 2777–2780.
[15] a) L. Grill, M. Dyer, L. Lafferentz, M. Persson, M. V. Peters, S. Hecht, *Nat. Nanotechnol.* **2007**, *2*, 687–691; b) M. Kolmer, A. A. A. Zebari, J. S. Prauzner-Bechcicki, W. Piskorz, F. Zasada, S. Godlewski, B. Such, Z. Sojka, M. Szymonski, *Angew. Chem. Int. Ed.* **2013**, *52*, 10300–10303; *Angew. Chem.* **2013**, *125*, 10490–10493; c) J. Cai, P. Ruffieux, R. Jaafar, M. Bieri, T. Braun, S. Blankenburg, M. Muoth, A. P. Seitsonen, M. Saleh, X. Feng, K. Müllen, R. Fasel, *Nature* **2010**, *466*, 470–473.
[16] a) N. Pavliček, B. Schuler, S. Collazos, N. Moll, D. Perez, E. Guitian, G. Meyer, D. Peña, L. Gross, *Nat. Chem.* **2015**, *7*, 623–628; b) B. Schuler, S. Fatayer, F. Mohn, N. Moll, N. Pavliček, G. Meyer, D. Peña, L. Gross, *Nat. Chem.* **2016**, *8*, 220–224; c) N. Pavliček, A. Mistry, Z. Majzik, N. Moll, G. Meyer, D. J. Fox, L. Gross, *Nat. Nanotechnol.* **2017**, *12*, 308–311; d) S. Zint, D. Ebeling, T. Schlöder, S. Ahles, D. Mollenhauer, H. A. Wegner, A. Schirmeisen, *ACS Nano* **2017**, *11*, 4183–4190; e) N. Pavliček, Z. Majzik, S. Collazos, G. Meyer, D. Perez, E. Guitian, D. Peña, L. Gross, *ACS Nano* **2017**, *11*, 10768–10773.

[17] a) J. Repp, G. Mayer, S. M. Stojkovic, A. Gourdon, C. Joachim, *Phys. Rev. Lett.* **2005**, *94*, 026803; b) S. Godlewski, H. Kawai, M. Kolmer, R. Zuzak, A. M. Echavarren, C. Joachim, M. Szymonski, M. Saeys, *ACS Nano* **2016**, *10*, 8499 – 8507; c) S. Godlewski, M. Kolmer, M. Engelund, H. Kawai, R. Zuzak, A. Garcia-Lekue, M. Saeys, A. M. Echavarren, C. Joachim, D. Sanchez-Portal, M. Szymonski, *Phys. Chem. Chem. Phys.* **2016**, *18*, 3854.

[18] a) L. Gross, F. Mohn, N. Moll, P. Liljeroth, G. Meyer, *Science* **2009**, *325*, 1110 – 1114; b) D. G. De Oteyza, P. Gorman, Y.-C. Chen, S. Wickenburg, A. Riss, D. J. Mowbray, G. Etkin, Z. Pedramrazi, H.-Z. Tsai, A. Rubio, M. F. Crommie, *Science* **2013**, *340*, 1434 – 1437; c) F. Albrecht, N. Pavliček, C. Herranz-Lancho, M. Ruben, J. Repp, *J. Am. Chem. Soc.* **2015**, *137*, 7424 – 7428; d) S. Kawai, S. Saito, S. Osumi, S. Yamaguchi, A. S. Foster, P. Spijker, E. Meyer, *Nat. Commun.* **2015**, *6*, 8098; e) A. Riss, A. Pérez Paz, S. Wickenburg, H.-Z. Tsai, D. G. De Oteyza, A. J. Bradley, M. M. Ugeda, P. Gorman, H. S. Jung, M. F. Crommie, A. Rubio, F. R. Fischer, *Nat. Chem.* **2016**, *8*, 678 – 683.

[19] L. E. Dinca, C. Fu, J. M. MacLeod, J. Lipton-Duffin, J. L. Brusso, C. E. Szalacs, D. Ma, D. F. Perepichka, F. Rosei, *ACS Nano* **2013**, *7*, 1652 – 1657.

[20] M. Zugermeier, M. Gruber, M. Schmid, B. P. Klein, L. Ruppenthal, P. Müller, R. Einholz, W. Hieringer, R. Berndt, H. F. Bettinger, J. M. Gottfried, *Nanoscale* **2017**, *9*, 12461.

[21] J. Urgel, H. Hayashi, M. Di Giovannantonio, C. A. Pignedoli, S. Mishra, O. Deniz, M. Yamashita, T. Dienel, P. Ruffieux, H. Yamada, R. Fasel, *J. Am. Chem. Soc.* **2017**, *139*, 11658 – 11661.

[22] J. Krüger, N. Pavliček, J. M. Alonso, D. Pérez, E. Guitián, T. Lehmann, G. Cuniberti, A. Groudon, G. Meyer, L. Gross, F. Moresco, D. Peña, *ACS Nano* **2016**, *10*, 4538 – 4542.

[23] J. Krüger, F. Eisenhut, J. M. Alonso, T. Lehmann, E. Guitián, D. Pérez, D. Skidin, F. Gamaleja, D. A. Ryndyk, C. Joachim, D. Peña, F. Moresco, G. Cuniberti, *Chem. Commun.* **2017**, *53*, 1583 – 1586.

[24] J. Krüger, F. Garcia, F. Eisenhut, D. Skidin, J. M. Alonso, E. Guitián, D. Pérez, G. Cuniberti, F. Moresco, D. Peña, *Angew. Chem. Int. Ed.* **2017**, *56*, 11945 – 11948; *Angew. Chem.* **2017**, *129*, 12107 – 12110.

[25] A. J. Athans, J. B. Briggs, W. Jia, G. P. Miller, *J. Mater. Chem.* **2007**, *17*, 2636 – 2641.

[26] R. Dorel, P. R. McGonigal, A. M. Echavarren, *Angew. Chem. Int. Ed.* **2016**, *55*, 11120 – 11123; *Angew. Chem.* **2016**, *128*, 11286 – 11289.

[27] R. Zuzak, R. Dorel, M. Krawiec, B. Such, M. Kolmer, M. Szymonski, A. M. Echavarren, S. Godlewski, *ACS Nano* **2017**, *11*, 9321 – 9329.

[28] See Supporting Information for details.

[29] W.-H. Soe, C. Manzano, A. De Sarkar, N. Chandrasekhar, C. Joachim, *Phys. Rev. Lett.* **2009**, *102*, 176102.

[30] While hydroacenes **1a**–**c** are stable under ambient conditions, precursors **1d**,**e** were found to be air sensitive.

[31] a) B. Hajgató, M. S. Deleuze, D. J. Tozer, F. De Proft, *J. Chem. Phys.* **2008**, *129*, 084308; b) A. Botelho, Y. Shin, J. Liu, X. Lin, *PLoS ONE* **2014**, *9*, e86370.

[32] H. Meier, U. Stalmach, H. Kolshorn, *Acta Polym.* **1997**, *48*, 379 – 384.

[33] a) J. M. Garcia-Lastra, C. Rostgaard, A. Rubio, K. S. Thygesen, *Phys. Rev. B* **2009**, *80*, 245427; b) J. B. Neaton, M. S. Hybertsen, S. G. Louie, *Phys. Rev. Lett.* **2006**, *97*, 216405.

Manuscript received: February 14, 2018
Accepted manuscript online: May 23, 2018
Version of record online: June 7, 2018

